

G. G. Diachenko¹,
orcid.org/0000-0001-9105-1951,
G. Schullerus²,
orcid.org/0000-0001-9740-9213,
A. Dominic²,
orcid.org/0000-0001-6872-1814,
O. O. Aziukovskiy¹,
orcid.org/0000-0003-1901-4333

1 – Dnipro University of Technology, Dnipro, Ukraine,
e-mail: diachenko.g@nmu.one
2 – Reutlingen University, Reutlingen, Germany

ENERGY-EFFICIENT PREDICTIVE CONTROL FOR FIELD-ORIENTATION INDUCTION MACHINE DRIVES

Purpose. To improve the efficiency of the closed-cycle operation of the field-orientation induction machine in dynamic behavior when load conditions are changing, considering the nonlinearities of the main inductance.

Methodology. The optimal control problem is defined as the minimization of the time integral of the energy losses. The algorithm observed in this paper uses the Matlab/Simulink, dSPACE real-time interface, and C language. Handling real-time applications is made in ControlDesk experiment software for seamless ECU development.

Findings. A discrete-time model with an integrated predictive control scheme where the optimization is performed online at every sampling step has been developed. The optimal field-producing current trajectory is determined, so that the copper losses are minimized over a wide operational range. Additionally, the comparison of measurement results with conventional methods is provided, which validates the advantages and performance of the control scheme.

Originality. To solve the given problem, the information vector on the current state of the coordinates of the electromechanical system is used to form a controlling influence in the dynamic mode of operation. For the first time, the formation process of controls has considered the current state and the desired future state of the system in the real-time domain.

Practical value. A predictive iterative approach for optimal flux level of an induction machine is important to generate the required electromagnetic torque and to reduce power losses simultaneously.

Keywords: *predictive control, energy efficiency, dynamic operation, real-time implementation*

Introduction. In the course of continuous improvement of the technologies and their diffusion throughout the industry and society, more severe becomes the problem of global energy conservation. It is connected with the increase in electricity consumption in industry and households as well as the related need for the construction and commissioning of new energy capacities due to a gradual shift from fossil fuel to electric vehicles. Leading by example, Norway promotes the use of electric vehicles with measurable success. It is safe to say that electric mobility will be a significant subject during the next years.

Literature review. Considering electric vehicles in general, a few obvious advantages, as well as disadvantages when comparing them to the solution based on the combustion engines, can be noticed. The functional principle of the electric propulsion system provides a clear advantage in the efficiency of the system. On the other hand, to achieve the full potential of an electric propulsion system, the energy mix in today's power generation must be changed to a more sustainable system by increasing the number of regenerative energy sources [1]. However, one of the significant disadvantages is the relatively low energy density of today's batteries, which results from the complex development in battery science [2]. By using a high-cost permanent magnet or separately excited synchronous machines, the efficiency can reach up to 95 % or more, which is

about three times higher than the efficiency of a combustion machine. In contrast, induction machines have high performance, high reliability, robustness, and low cost at lower efficiency [3]. Thus, the question of increasing the energy efficiency of these machines is a widely discussed topic in research and development nowadays. A large number of publications addressed the problem of induction machine losses minimization in the steady-state [4]. However, in applications like an electric vehicle, an electric machine will be mostly operated in dynamic mode, especially in urban areas, with changing torque and speed often up to current and voltage limits. Compared to the number of scientific papers for the steady-state mode, only a small part of them is addressing the question of energy efficiency in dynamics.

Unsolved aspects of the problem. The reduction of power loss in the dynamic mode of operation is usually treated using offline numerical investigation on a PC, based on full knowledge of the load torque and speed profile. Then, the templates are generated to enable an online implementation. These methods give a significant improvement compared to the operation under constant flux reference. However, offline optimization is not feasible in such type of application because the precalculated optimal trajectories cover only certain operating conditions. Moreover, the solution of the optimization problem is complicated by the fact that no simple closed-form solution could be obtained, resulting in the need to find a real-time implementable numerical solution in the inverter at high sampling rates.

Purpose. The main contribution of the current paper is to verify and validate experimentally the ideas initially presented in [5, 6] for the closed-cycle operation of field-orientation induction machine drive considering the influence of a variable main inductance. Recently, more and more mechanisms that are constantly operating in dynamic mode with variable speed and variable, often unknown beforehand load. These include, for example, conveyor lines, delta robots, electric vehicles and others. Thus, the proposed solution covers a substantial part of the possible applications of an induction motor.

Results. To illustrate the proposed solution, the following two subsections describe the motor model and losses representation used in this paper. Then, the optimal control problem (OCP) formulation to obtain a real-time implementable solution in dynamic operation is discussed. Subsequently, the simulation results are illustrated for a particular speed and load torque profile, followed by measurements. Finally, experimental results conclude the paper.

Motor model. For the modeling of an induction motor the Γ -inverse model is used, all variables are transformed from the three-phase system (abc) to an orthogonal amplitude invariant dq reference frame with a direct (d) and a quadrature (q) axis. The field orientation is made along the rotor flux linkage Ψ_2 , i.e. the flux linkage phasor is aligned with the d -axis of the synchronously rotating coordinate frame. The state-space model of the motor dynamics is represented by the following differential equation system

$$\frac{d}{dt}i_{1d} = \frac{R_2}{L_m L_\sigma} \Psi_2 - \frac{1}{L_\sigma} (R_1 + R_2) i_{1d} + \omega_1 i_{1q} + \frac{u_{1d}}{L_\sigma}; \quad (1)$$

$$\frac{d}{dt}i_{1q} = -\frac{\omega_2}{L_\sigma} \Psi_2 - \frac{1}{L_\sigma} (R_1 + R_2) i_{1q} - \omega_1 i_{1d} + \frac{u_{1q}}{L_\sigma}; \quad (2)$$

$$\frac{d}{dt} \Psi_2 = -\frac{R_2}{L_m} \Psi_2 + R_2 i_{1d}; \quad (3)$$

$$\frac{d}{dt} \omega_2 = Z_p \frac{(T_e - T_{load})}{J}. \quad (4)$$

The electromagnetic torque is given by

$$T_e = \frac{3}{2} Z_p \Psi_2 i_{1q}. \quad (5)$$

The equations (1–5) have the following denotations: i_{1d} and i_{1q} are the stator current phasor components, ω_1 represents the stator angular frequency and ω_2 represents the rotor shaft mechanical angular velocity, T_e and T_{load} are motor and load torque, Z_p is the number of pole pairs, J is the moment of inertia, and finally u_{1d} and u_{1q} are the stator voltage phasor components, R_1 and R_2 are the stator and rotor resistances, L_σ is the stray inductance and L_m denotes the main inductance.

Main inductance saturation. In practice, the modeling of an induction machine as a linear object is inadequate even for nominal operating conditions because of magnetic saturation. The main inductance data is obtained experimentally on the test bench. The measured data points are approximated by a 5th order polynomial function using Curve Fitting Toolbox from the MATLAB environment

$$L_m(i_{1d}) = P_1 i_{1d}^5 + P_2 i_{1d}^4 + P_3 i_{1d}^3 + P_4 i_{1d}^2 + P_5 i_{1d} + P_6.$$

Power loss. The input power P_{in} can be represented as a sum of the output mechanical power P_{out} and the power loss P_{loss}

$$P_{in} = P_{loss} + \omega(t) T_e(t). \quad (7)$$

The paper is focused on copper losses. The core losses are not considered. Note, however, that a reduction of the flux level in energy-efficient mode will also reduce the core losses. In addition, core losses can be included at the expense of higher computational demands. From the physical interpretation

of the equivalent circuit, the instantaneous power losses from (7) in the induction machine are given by

$$P_{loss} = \frac{3}{2} R_1 (i_{1d}^2 + i_{1q}^2) + \frac{3}{2} R_2 (i_{2d}^2 + i_{2q}^2), \quad (8)$$

where i_{1d} , i_{1q} , and i_{2d} , i_{2q} are the stator and rotor current phasor components, respectively. Under rotor flux orientation, the components of the rotor current phasor are defined as

$$i_{2d} = \frac{1}{L_m(i_{1d})} \Psi_2 - i_{1d} = -\frac{1}{R_2} \Psi_2; \quad (9)$$

$$i_{2q} = -i_{1q}. \quad (10)$$

Substitution of (9) and (10) into (8) results in

$$P_{loss} = \frac{3}{2} (R_1 + R_2) (i_{1d}^2 + i_{1q}^2) + \frac{3}{2} R_2 \left(\frac{1}{L_m^2(i_{1d})} \Psi_2^2 - \frac{2}{L_m(i_{1d})} \Psi_2 i_{1d} \right). \quad (11)$$

When using the field-oriented control approach, the torque-producing current i_{1q} is determined by the mechanical torque on the motor shaft. Given that in the steady-state mode of operation, the machine develops a torque equal to the load torque $T_e = T_{load}$, from (5) the steady-state value for i_{1q} , in this case, taking into account an appropriate steady-state rotor flux value Ψ_2 , is written as follows

$$i_{1q} = \frac{2}{3} \frac{T_e}{Z_p \Psi_2}. \quad (12)$$

Substituting (12) into (11) results in

$$P_{loss} = \underbrace{\frac{3}{2} R_1 i_{1d}^2 + \frac{2}{3} (R_1 + R_2) \frac{T_e^2}{Z_p^2 \Psi_2^2}}_{P_{loss}^{ss}} + \underbrace{\frac{3}{2} R_2 \left(i_{1d}^2 + \frac{1}{L_m^2(i_{1d})} \Psi_2^2 - \frac{2}{L_m(i_{1d})} \Psi_2 i_{1d} \right)}_{P_{loss}^{dyn}}, \quad (13)$$

where the first part P_{loss}^{ss} represents the power losses in the steady-state mode of operation while the second part P_{loss}^{dyn} contains transient power losses due to i_{1d} . From (13) it can be noticed that P_{loss}^{ss} depends on i_{1d} as well as L_m , R_1 , R_2 .

Given that $P_{loss}^{ss} = f(i_{1d})$ the exploration of the minimum can be done. Taking the derivative of the first part of (13), that is P_{loss}^{ss} , with respect to i_{1d} gives us the optimal value of the field-producing current in the steady-state mode with constant L_m .

$$i_{1d}^*(T_e) = \sqrt{\frac{2}{3} \frac{T_e}{Z_p L_m} \sqrt{\frac{R_1 + R_2}{R_1}}}. \quad (14)$$

The dependence of the power loss on the field-producing current i_{1d} is given by expression (13), and it can be clearly understood that for each level of the load torque on the motor shaft, there is a corresponding optimal field-producing current as given in (14), at which the minimum power loss is achieved.

The minimum of power loss can be calculated by substituting (14) in (13)

$$P_{loss}^* = T_e \frac{R_1 + R_1 \xi^2 + R_2 \xi^2}{Z_p L_m \xi},$$

where $\xi = \sqrt{R_1 / (R_1 + R_2)}$.

The use of the optimal field-producing current allows obtaining a theoretically constant efficiency of an induction motor drive at any mechanical load torque in steady-state. Considering (7) and (15) from the ratio of the useful work per-

formed by a machine or in a process to the total energy expended or heat taken in, the efficiency is

$$\eta = \frac{P_{out}}{P_{in}} = \frac{P_{out}}{P_{out} + P_{loss}} = \frac{T_e \omega_2}{T_e \omega_2 + P_{loss}} = \frac{1}{1 + \zeta / \omega_2}, \quad (16)$$

where $\zeta = (R_1 + R_1 \xi^2 + R_2 \xi^2) / (Z_p L_m \xi)$ from (15).

The efficiency calculations using (16) were made for two cases of induction machine power supply from a frequency converter operating in vector mode with an optimal and rated field-producing current setpoints. The plot of the efficiency versus load torque on the motor shaft is shown in Fig. 1.

The dependence in Fig. 1 allows comparing the difference between the efficiency of an induction machine operating with constant field-producing current setpoint at the rated level and with an optimized flux level trajectory. In addition, the average effectiveness of applying an optimized trajectory could be retrieved. From this data, the following trend can be traced: the smaller the torque is, the greater the gain in the effectiveness from the optimized trajectory is.

Torque profile. From (13), it can be clearly seen that the required torque trajectory affects the power losses of the electric machine. The torque trajectory is considered to have first-order behavior in [7]. In this paper, the torque is taken as an output of the speed controller [8].

The dynamics of the stator currents is significantly faster than the dynamics of the flux linkage and the speed. Hence, it is assumed here that the speed controller can ensure the commanded torque value T_e instantaneously for a given rotor flux linkage Ψ_2 if the current phasor is maintained in reasonable bounds. In such a case, the dynamics of the speed and current controllers can be disregarded. The reduced motor model to be used further in this paper in the optimization problem can be rewritten by (3, 5). The motor torque T_e in the control scheme is represented as a sum of the value commanded by the speed controller T_{ec} and the feedforward torque T_{effw} . In this regard, the motor torque T_e is generated in two ways:

1. The main contribution to the T_e is retrieved from the feedforward control signal T_{effw} due to a speed ramp. The *PI*-controller accounts only for the model uncertainties.

2. The *PI*-controller generates the torque T_e due to a change in the mechanical load torque T_{load} .

Optimization problem formulation. The overall objective of this paper is the optimization of motor efficiency for dynamic operation, that is, for the situations when the motor torque T_e changes from initial steady-state value T_0 to a final steady-state value T_1 and/or for changing speeds. The speed reference in the form of a speed ramp $\omega_{2, ref}(t)$ in a time interval $t \in [t_0, t_f]$ is considered here. The efficiency is evaluated based on the overall energy losses. Therefore, the performance index includes power losses solely and is formulated as follows

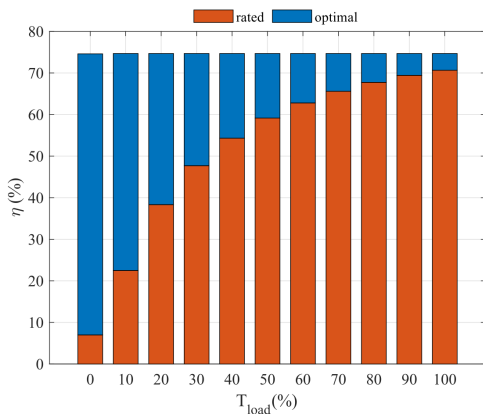


Fig. 1. Dependence $\eta(T_{load})$ for a 370 W motor with power supply from a frequency converter for optimal and rated flux-generating current setpoints

$$J = \int_{t_0}^{t_f} P_{loss}(t) dt. \quad (17)$$

The optimal field-producing current trajectory is a conditional minimum of the functional (17) under the constraint given by the dynamics of the flux linkage (3), including the main inductance L_m saturation effect (6) and the following boundary conditions

$$\Psi_2(t_0) = L_m(i_{1d}^*(T_0))i_{1d}^*(T_0); \quad (18)$$

$$\Psi_2(t_f) = L_m(i_{1d}^*(T_1))i_{1d}^*(T_1), \quad (19)$$

as well as constraints $\sqrt{u_{1d}^2 + u_{1q}^2} \leq U_s$, $\sqrt{i_{1d}^2 + i_{1q}^2} \leq I_s$.

U_s is the maximum length of the VSI output voltage phasor, which depends on the DC link voltage of the inverter. The voltages are commonly restricted to the dashed circle to reduce torque ripples. I_s is the current limit given by the maximum length of the VSI output current phasor and/or motor maximum current.

The Hamiltonian for this problem is given by [6]

$$H = \dot{J} + \lambda \dot{\Psi}_2, \quad (20)$$

where $\lambda \in R^{N_s}$ is the adjoint state or costate. From the Pontryagin's Maximum Principle, the first-order optimality condition can be expressed as a system of PDEs

$$\frac{\partial H}{\partial \Psi_2} = -\dot{\lambda}, \quad \frac{\partial H}{\partial i_{1d}} = 0, \quad \frac{\partial H}{\partial \lambda} = \dot{\Psi}_2. \quad (21)$$

There is no closed-form solution to this problem due to the presence of the component of nonlinear nature $L_m(i_{1d})$ in (21). Therefore, expression (20) is subjected to a numerical approach. The implementation of the dynamic trajectory optimization requires the consideration of the system state dynamics and constraints along with the boundary conditions (18, 19). In [9] a similar problem was solved, and an analytical solution for optimal rotor flux in the form of a time-varying law for finite optimization horizon was obtained from offline OCP. In the implementation of our problem, the GRAMPC Toolbox will be used [10]. The solution is based on grampc v1.0. The model predictive approach was further adapted to real-time loss-minimizing flux level control for closed-cycle operation of field-orientation induction machine drives under torque changes in MATLAB and dSPACE. For implementation purposes, the continuous-time system of the equations (3, 5) is discretized with the sampling time T_s and $t = kT_s$.

Objective functional. From the discretization of the performance index (17), the discrete-time version is obtained

$$J_d = \sum_{k=1}^N P_{loss}(k), \quad (22)$$

where $P_{loss}(k)$ is the discretized instantaneous power loss at the sampling instants. By substituting the equation (13) in (22), we get

$$J_d = \frac{3}{2} \sum_{k=1}^N R_1 i_{1d}^2(k) + \frac{2}{3} \sum_{k=1}^N (R_1 + R_2) \frac{T_e^2(k)}{Z_p^2 \Psi_2^2(k)} + \frac{3}{2} \sum_{k=1}^N R_2 \left(i_{1d}^2(k) + \frac{1}{L_m^2(i_{1d}(k))} \Psi_2^2(k) \right) - \frac{3}{2} \sum_{k=1}^N \frac{2R_2}{L_m(i_{1d}(k))} \Psi_2(k) i_{1d}(k).$$

The state discretization is implemented using the forward Euler method. Calculation of the system's future state is done

explicitly without the need to solve algebraic equations. For the forward method, first, a step size h is chosen

$$h = \frac{T}{N},$$

where T is the simulation time, and N is the number of discretization points. The size h determines the accuracy of the solution, meaning that as the step size decreases, the error between the actual and the approximation reduces as well. This method produces a series of line segments, which thereby approximates the solution curve. Let t_k be a sequence in time at the k^{th} sample instant and y_k is the solution at $t = t_k$

$$t_{k+1} = t_k + h.$$

To get y_{k+1} from (t_k, y_k) , a differential equation is used. It is assumed that the next point (t_{k+1}, y_{k+1}) lies on the line through the point (t_k, y_k) with the slope $f(t_k, y_k)$. From this reasoning, the formula for the slope of a line looks as follows

$$y_{k+1} = y_k + f(t_k, y_k)h.$$

Thus, knowing the value of $y_0 = f(t, y)$ at the initial guess (t_0, y_0) allows defining the solution. The initial guess can be determined from the given initial state. It is considered that the motor is in a steady-state prior to any speed ramps and/or load change.

Simulation results. The simulation results obtained with the optimization problem discussed in the previous section are illustrated in Fig. 2. For the simulation purposes, the motor is initialized to operate at a constant speed $\omega_{2,1}$ and a given load torque $T_{load} = 20\% T_N$ Nm before $t = 0$ s. At time $t = 0.2$ s a speed ramp to $\omega_{2,2}$ in the interval $t \in [0.2, 0.4]$ s is commanded. The dynamics of T_e is determined by the controller parameters. However, the focus is not on discussing the speed controller dynamics but on illustrating the solution of the power loss minimization problem by means of predictive flux control. The considered motor has a rated power $P_r = 370$ W, a nominal torque $T_N = 2.59$ Nm and a rated speed of rotation $N_r = 1370$ rpm. The additional motor and simulation parameters are specified in Table. The load torque is given by the expression from [11]

$$T_{load}(t) = \begin{cases} 20\% T_N, & t < 0.2s, \quad t \geq 0.8s \\ 40\% T_N, & 0.2s \leq t < 0.6s \\ 60\% T_N, & 0.6s \leq t < 0.8s \end{cases}.$$

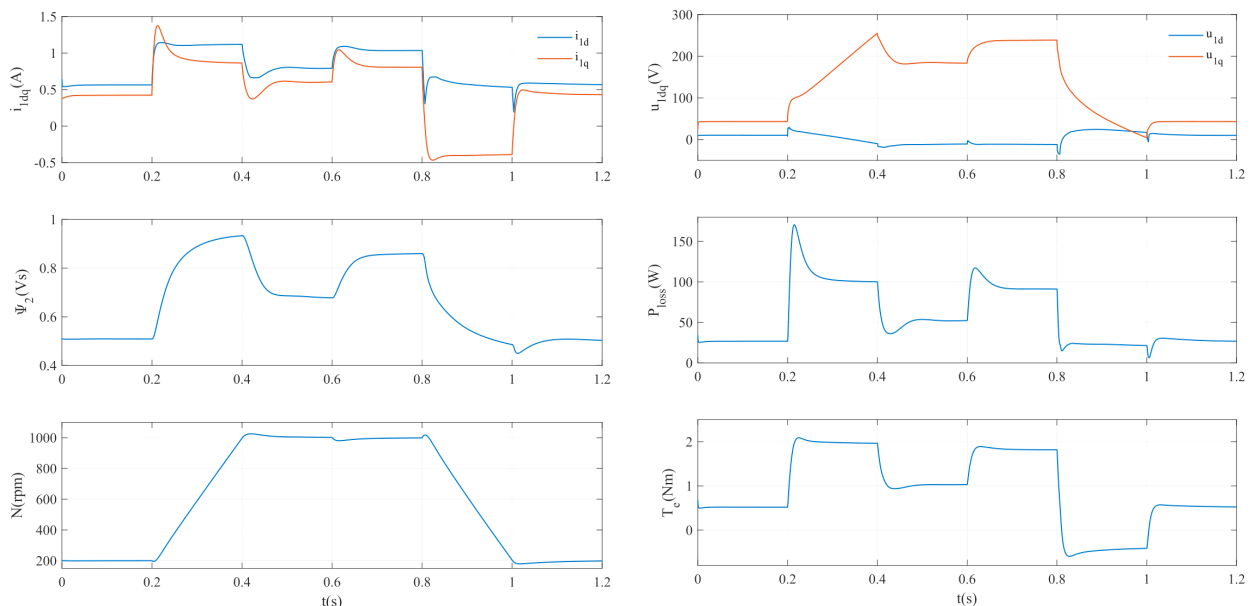


Fig. 2. Optimization results

The given moment of inertia J is the overall value for the system under test consisting of the induction motor, load machine, the coupling between them, and the torque sensor. The load torque transition from one steady-state to another steady-state value is assumed to be stepwise. Fig. 2 illustrates the results of the solution of the optimization problem from the MATLAB/Simulink environment with $t_0 = 0.2$ and $t_f = 1.2$ s. The power losses are calculated with (11) using the stator current components i_{1d} , i_{1q} , the rotor flux Ψ_2 , and other motor parameters from Table. The rotor flux Ψ_2 before the ramp-up equals the optimal steady-state value obtained as a result of the multiplication of (14) by $L_m(i_{1d}(T_e))$. With speed increase, the motor torque T_e also increases, resulting in new optimal rotor flux Ψ_2 and corresponding trajectory for $i_{1d}(T_e)$. When the speed setpoint is reached, the dynamic torque $T_{dyn} = T_e - T_{load}$ becomes 0, thus resulting in new optimal rotor flux Ψ_2 and corresponding trajectory for $i_{1d}(T_e)$ again. This behavior can be noticed in the stator voltage components u_{1d} and u_{1q} . In contrast to [12], the flux changes simultaneously with the torque change.

Experimental results. The results obtained in section V are now validated on the test bench with a 370 W-motor shown in Fig. 3. The inverter for the motor under test was modified so that the controller hardware in the inverter was bypassed and the PWM-signals of the power stage, as well as the internal current and dc-link-voltage sensors, could be accessed. The modified field-oriented control algorithm and the grampc approach are implemented in a dSPACE ds1104-system. The load is provided by a permanent magnet synchronous machine controlled by a standard inverter. The torque is measured using a torque sensor. The measurement results are presented in Fig. 4.

Three different approaches for controlling i_{1d} during speed ramps and load transients are compared in the sequel:

- Without optimization: i_{1d} is set to a const rated value.
- Suboptimal: Filtered stepwise i_{1d} profile from [5].
- With optimization: The optimal grampc solution discussed.

The reference for the torque-producing current $i_{1q,ref}$ is calculated by rewriting (5) and based on the rotor flux linkage Ψ_2 obtained from the first-order model of flux estimator. The PWM-frequency is 4 kHz. The MPC block is run for the test at 1 kHz. The power losses illustrated in Fig. 5 are calculated with (11) as in the previous section. The field-producing cur-

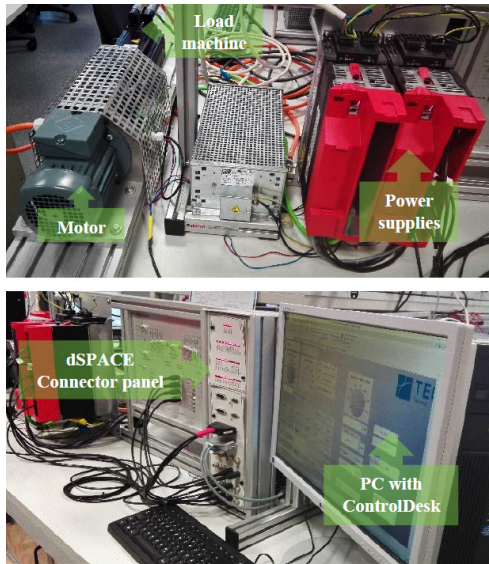


Fig. 3. Test bench

Motor data [11]

Table

Engine parameters			
R_1	27.8 Ω	R_2	20 Ω
T_N	2.59 Nm	L_σ	0.142 H
Z_p	2	J	$22 \cdot 10^{-4}$ kgm ²
P_1	-0.669	P_2	3.606
P_3	-6.622	P_4	4.415
P_5	-0.743	P_6	0.754
$\omega_{2,1}$	20.94 rad/s (200 rpm)	$\omega_{2,2}$	104.7 rad/s (1000 rpm)

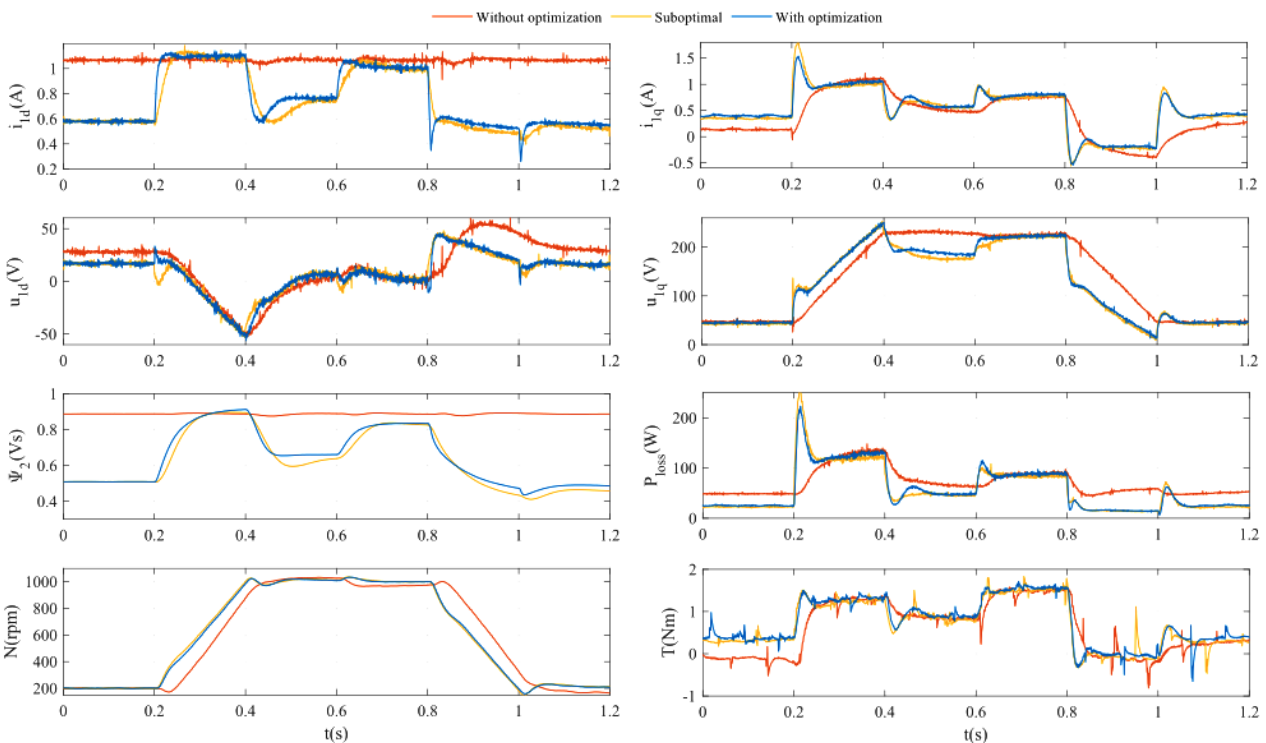


Fig. 4. Measurements

rent i_{ld} trajectory in the optimized case corresponds to the trajectory obtained in the previous section. The possible slight mismatch in the torque-producing current is related to neglecting the core losses and simplified friction torque. In the steady-state part loaded mode of operation, the use of optimal flux trajectory leads to a reduction of the energy losses. At a time when the load torque step is applied as well as/or speed ramp-up reference, an overshoot in the power losses can be observed for both suboptimal and optimal solutions in contrast to the nominal case due to higher mechanical power requirements to increase the flux to the new optimal level at initially lower flux linkage.

In Fig. 6 a comparison of energy losses which is the integral of the power losses for the time interval $t \in [0, 1.2]$ s is illustrated.

It can be seen that the results for the filtering technique and predictive approach give almost the same result, which confirms the numerical and simulation study [5].

One main difference, however, is that the main inductance saturation (that is changing rotor time constants) was not considered in the filtering approach. Consequently, the steady-state flux reference is a bit lower than optimal, resulting in lower power loss.

The abnormal speed profile for the nominal case might be connected to the fact that the load torque was not applied before speed ramp-up and step increase in the load.

Conclusions. The current paper presented energy-efficient control for the rotor flux linkage in the framework of the field-oriented control structure that minimizes the energy losses under torque step changes. In this work, the trajectories are computed in a real-time procedure. The results illustrate that an optimal solution to the loss minimization problem with a variable inductance gives acceptable results. The optimal solution was compared to the offline numerically obtained suboptimal solution of the optimization problem using the filtering of step-like reference for the conventional flux controller. In addition, experimental measurements illustrate the reduction of energy losses compared to the nominal case.

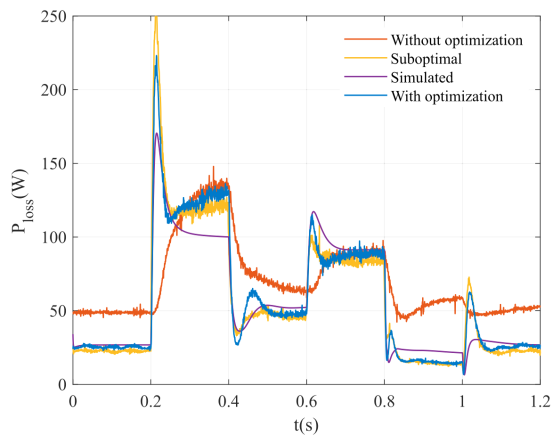


Fig. 5. Comparison of power losses

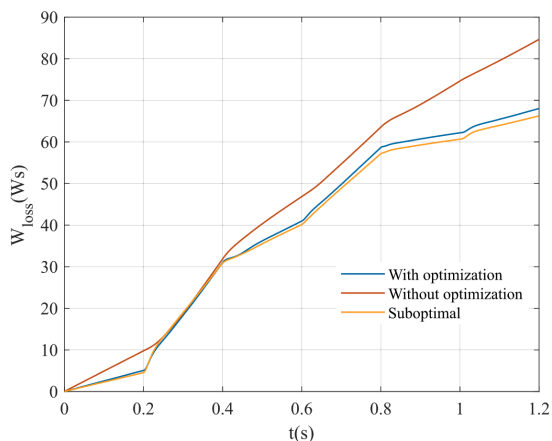


Fig. 6. Comparison of energy losses

Acknowledgements. This work was supported by the “DAAD Ostpartnerschaften” scholarship program and by the Baden-Württemberg Foundation.

References.

1. Beshta, A., Beshta, A., Balakhontsev, A., & Khudolii, S. (2019). Performances of asynchronous motor within variable frequency drive with additional power source plugged via combined converter. *2019 IEEE 6th International Conference on Energy Smart Systems (ESS)*, (pp. 156-160). Kyiv, Ukraine. <https://doi.org/10.1109/ESS.2019.8764192>.
2. Koriashkina, L. S., Deryugin, O. V., Fedoriachenko, S. O., Cheberiyachko, S. I., & Vesela, M. A. (2019). On determining productive capacity of EV traction battery repair area. *Naukovyi Visnyk Natsionalnoho Hirnychoho Universytetu*, (5), 113-121. <https://doi.org/10.29202/nvngu/2019-5/17>.
3. Beshta, O. S., Fedoreiko, V. S., Balakhontsev, O. V., & Khudolii, S. S. (2013). Dependence of electric drive's thermal state on its operation mode. *Naukovyi Visnyk Natsionalnoho Hirnychoho Universytetu*, (6), 67-72.
4. Hannan, M. A., Ali, J. A., Mohamed, A., & Hussain, A. (2018). Optimization techniques to enhance the performance of induction motor drives: A review. *Renewable and Sustainable Energy Reviews*, 81, 1611-1626. <https://doi.org/10.1016/j.rser.2017.05.240>.
5. Diachenko, G., & Schullerus, G. (2015). Simple dynamic energy efficient field oriented control in induction motors. *Proceedings of the 18th International Symposium on Power Electronics EE2015*, (pp. 1-5). Novi Sad, Serbia. Retrieved from https://elprivod.nmu.org.ua/ua/articles/Дяченко_Session8-03615.pdf.
6. Diachenko, G., Aziukovskyi, O., Rogoza, M., & Yaki-mets, S. (2019). Optimal field-oriented control of an induction

motor for loss minimization in dynamic operation. *2019 IEEE International Conference on Modern Electrical and Energy Systems (MEES)*, (pp. 94-97). Kremenchuk, Ukraine. <https://doi.org/10.1109/MEES.2019.8896455>.

7. Stumper, J., Dötlinger, A., & Kennel, R. (2013). Loss minimization of induction machines in dynamic operation. *IEEE Transactions on Energy Conversion*, 28(3), 726-735. <https://doi.org/10.1109/TEC.2013.2262048>.

8. Borisevich, A., & Schullerus, G. (2016). Energy efficient control of an induction machine under torque step changes. *IEEE Transactions on Energy Conversion*, 31(4), 1295-1303. <https://doi.org/10.1109/TEC.2016.2561307>.

9. Abdelati, R., & Mimouni, M. F. (2019). Optimal control strategy of an induction motor for loss minimization using Pontryaguin principle. *European Journal of Control*, 49, 94-106. <https://doi.org/10.1016/j.ejcon.2019.02.004>.

10. Käpernick, B., & Graichen, K. (2014). The gradient based nonlinear model predictive control software GRAMPC. *2014 European Control Conference (ECC)*, (pp. 1170-1175). Strasbourg, France. <https://doi.org/10.1109/ecc.2014.6862353>.

11. Diachenko, G. (2020). Rotor flux controller for induction machines considering main inductance saturation. *Problems of the regional energetics*, 3(47), 10-19. <https://doi.org/10.5281/zenodo.4018933>.

12. Dominic, A., Schullerus, G., & Winter, M. (2019). Optimal flux and current trajectories for efficient operation of induction machines. *2019 20th International Symposium on Power Electronics (Ee)*, (pp. 1-6). Novi Sad, Serbia. <https://doi.org/10.1109/PEE.2019.8923512>.

Енергоефективне прогнозне керування у векторно-керованому асинхронному електроприводі

Г. Г. Дяченко¹, Г. Шуллерус², А. Домінік²,
О. О. Азіюковський¹

1 – Національний технічний університет «Дніпровська політехніка», м. Дніпро, Україна, e-mail: diachenko.g@nmu.one;

2 – Ройтлінгенський університет, м. Ройтлінген, Німеччина

Мета. Підвищити енергоефективність векторно-керованого асинхронного електропривода під час перехідних процесів, коли змінюються умови навантаження, урахувавши ефект насичення магнітної індукції.

Методика. Задача оптимального керування визначається як мінімізація інтегралу втрат енергії. Алгоритм, що застосовується у цій роботі, використовує Matlab/Simulink, інтерфейс реального часу dSPACE та мову С. Обробка програм у режимі реального часу виконується в експериментальному програмному забезпеченні ControlDesk.

Результати. Розроблена дискретна модель з інтегрованою схемою на базі методу прогнозування, де оптимізація проводиться в режимі онлайн на кожному етапі вибірки. Оптимальна траєкторія струму намагнічування визначається таким чином, що втрати мінімізуються в широкому робочому діапазоні. Додатково надається порівняння результатів вимірювань зі звичайними методами, що підтверджує переваги та ефективність схеми управління.

Наукова новизна. Для вирішення заданої задачі використовується інформаційний вектор про поточний стан координат електромеханічної системи для формування керуючого впливу в динамічному режимі роботи. Уперше процес формування елементів керування враховує поточний стан і бажаний майбутній стан системи в області реального часу.

Практична значимість. Прогнозний ітеративний підхід для оптимального рівня потоку асинхронної машини важливий для створення необхідного електромагнітного крутного моменту та одночасного зменшення потужності втрат.

Ключові слова: прогнозне керування, енергоефективність, динамічний режим, реальний час

Энергоэффективное прогнозное управление в векторно-управляемом асинхронном электроприводе

Г. Г. Дяченко¹, Г. Шуллерус², А. Доминик²,
А. А. Азюковский¹

1 – Национальный технический университет «Днепровская политехника», г. Днепр, Украина, e-mail: diachenko.g@nmu.one

2 – Ройтлингенский университет, г. Ройтлинген, Германия

Цель. Повысить энергоэффективность векторно-управляемого асинхронного электропривода во время переходных процессов, когда меняются условия нагрузки, учитывая эффект насыщения магнитной индукции.

Методика. Задача оптимального управления определяется как минимизация интеграла потерь энергии. Алгоритм, применяемый в этой работе, использует Matlab/

Simulink, интерфейс реального времени dSPACE и язык С. Обработка программ в режиме реального времени выполняется в экспериментальном программном обеспечении ControlDesk.

Результаты. Разработана дискретная модель с интегрированной схемой на базе метода прогнозирования, где оптимизация проводится в режиме онлайн на каждом этапе выборки. Оптимальная траектория тока намагничивания определяется таким образом, что потери минимизируются в широком рабочем диапазоне. Дополнительно предоставляются сравнения результатов измерений с обычными методами, что подтверждает преимущества и эффективность схемы управления.

Научная новизна. Для решения заданной задачи используется информационный вектор о текущем состоянии координат электромеханической системы для формирования управляющего воздействия в динамическом режиме работы. Впервые процесс формирования элементов управления учитывает текущее состояние и желаемое будущее состояние системы в области реального времени.

Практическая значимость. Прогнозный итеративный подход для оптимального уровня потока асинхронной машины важен для создания необходимого электромагнитного крутящего момента и одновременного уменьшения мощности потерь.

Ключевые слова: прогнозное управления, энергоэффективность, динамический режим, реальное время

Recommended for publication by M. O. Aleksiev, Doctor of Technical Sciences. The manuscript was submitted 25.04.20.